TIME AND MATTER 2013 CONFERENCE

t&m Time and Matter
2013 Venice, Italy

Quantum Geometry and the Fermilab Holometer

C. STOUGHTON[1*], *for* The Fermilab Holometer Collaboration[2]

[1] *Fermi National Accelerator Laboratory*
[2] `http://holometer.fnal.gov`

Abstract: Recent theoretical work [1], [2], [3], [4] proposes a quantum aspect of geometry, with position operators obeying the commutator $[X_i, X_j] = i\ell'_P\epsilon_{ijk}X_k$. This leads to an uncertainty in transverse distance after propagating a distance D of $\langle x_\perp^2 \rangle = L\ell'_P$ with $l'_P \sim$ the Planck length. The Fermilab Holometer consists of two Michelson interferometers which search for macroscopic effects of this uncertainty.

Motivation

Reconciling the pillars of modern physics is not a new venture, but we propose here a new approach: to treat locations in spacetime with quantum operators. General relativity describes the dynamics of spacetime: Lorentz contraction, gravitation, and the accelerated expansion of the Universe. Using quantum operators for location may help us understand regimes where relativity and quantum mechanics meet.

Among several systems of natural units discussed by K. A. Tomlin [5] the Planck system most clearly describes this meeting place. From three physical constants $c, \hbar, G$, we derive:

$$\text{Length: } \ell_P = \sqrt{\frac{\hbar G}{c^3}} = 1.6 \times 10^{-35} \text{ meters} \tag{1}$$

$$\text{Time: } t_P = \sqrt{\frac{\hbar G}{c^5}} = 5.4 \times 10^{-44} \text{ seconds} \tag{2}$$

$$\text{Mass: } m_P = \sqrt{\frac{\hbar c}{G}} = 2.2 \times 10^{-8} \text{ kilograms} \tag{3}$$

* `stoughto@fnal.gov`

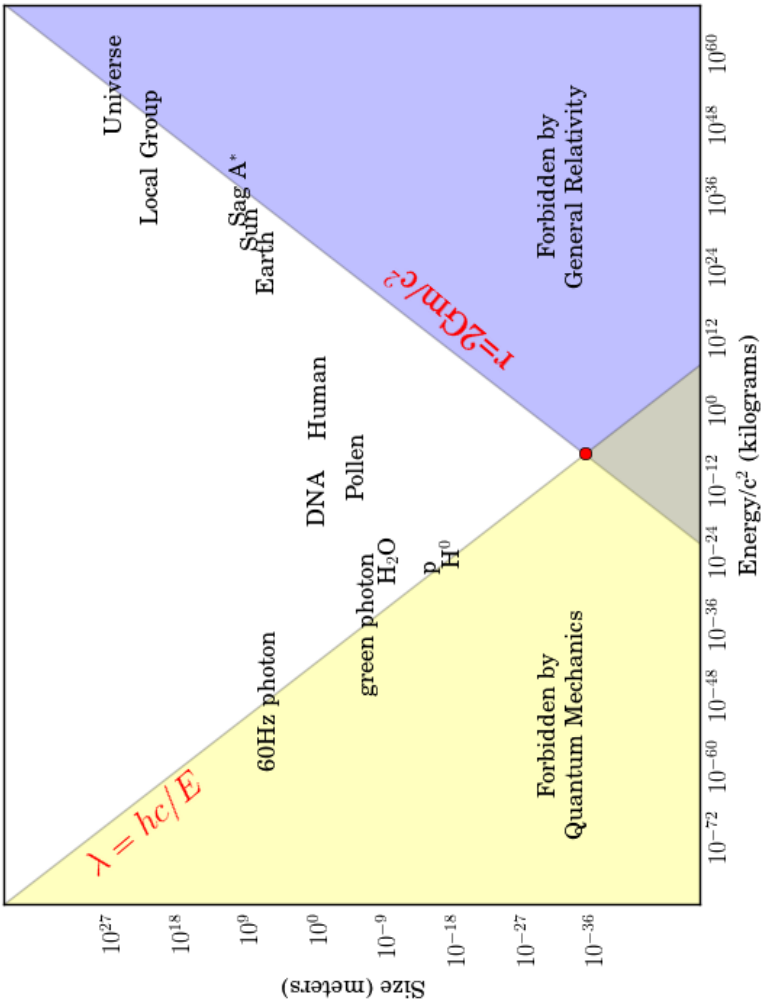

Figure 1: The size/energy relations for Quantum Mechanics and Relativity. The red dot indicates the scales where their effects are comparable.

A motivation for the theoretical work stems from the contrasting trend of size as a function of energy for relativity and quantum mechanics. Figure 1 illustrates this for the radius of a black hole $r = 2Gm/c^2$ and the wavelength of a photon $\lambda = hc/E$. Regions below these lines are forbidden. For example, an object with the mass of Sag A* (the black hole at the center of the Milky Way) 10^{36} kg, has a minimum possible radius $\sim 10^{12}$ m. A higher density (smaller radius for this mass) is not allowed by general relativity. On the other side of Figure 1 we have a "large" photon with frequency of 60 Hz. This wavelength is approximately the size of the Earth. Green photons (higher energy) have shorter wavelengths. Small particles with non-zero rest mass, such as water molecules, protons, or the recently-discovered Higgs boson, lie slightly above the $\lambda = hc/E$ line. The region below this line is forbidden by quantum mechanics. The two lines meet at an E/c^2 equal to the Planck mass 2.2×10^{-8} kg. Objects can have have a mass higher or lower than this mass. However, the length associated with this mass is identical for quantum mechanics and relativity: for a Planck mass $\lambda = hc/E$ and $r = 2Gm/c^2$ are both the Planck length, 1.6×10^{-35} meters. The Planck length is a fundamental length scale.

A second motivation for the new theoretical ideas comes from thermodynamics. The entropy of a system measures the number of ways that it could be arranged. As a system evolves in time entropy increases. Hawking noted [6] that the event horizon area of a black hole cannot decrease. Since this is similar to how entropy behaves, the simplest assumption is that the entropy of a black hole (S_{BH}) increases as the area of its event horizon. Beckenstein and Hawking worked out the constant of proportionality [7], defining the entropy of a black hole (or Beckenstein-Hawking entropy) to be

$$S_{BH} = 4\pi(R/2\ell_P)^2 \tag{4}$$

Naively, we expect the number of ways to organize things inside a region to increase as the volume of the region. Note here the surprise that it increases only as the surface area of the region: there are not as many ways to arrange a black hole as one might initially think.

The holographic principle generalizes from the special case of black holes to any region of space, described by Bousso [8]. A calculation by Verlinde [9] give the number of states in a sphere:

$$N_G(R) = 4\pi(R/\ell_P)^2. \tag{5}$$

Note that in Equations 4 and 5, the area of the surface that surrounds the region is expressed in units of the fundamental Planck length ℓ_P squared. Gerard 't Hooft describes the situation: *"Nature's book keeping system: the*

data can be written onto a surface, and the pen with which the data are written has a finite size."[10]

The third motivation of these theoretical ideas are considerations of geometry. Classical geometry is based on notions of points in space: locality is presumed. It is paradoxical, then, to use this geometry in quantum physics, which does not ascribe events to definite points. How does geometry work for quantum measurements? A standard architecture of physics has a dynamic spacetime which responds to particles and fields. These quantum particles and fields are defined on the "stage" of classical geometry. This accommodation explains all quantum mechanics (fundamental particle physics) experiments, as well as observations of the dynamics of spacetime, such as gravitational lensing (the deflection of light by mass) and spin-down of pulsars which are observed to lose energy at the rate predicted by gravitational radiation.

This collision of quantum mechanics and relativity leads us to consider a new part of the story. We will treat spacetime as a statistical behavior of a quantum system, and realize that states have new forms of spatially nonlocal entanglement.

Hypothesis

These considerations lead us to describe location with an operator which has the following commutator:

$$[X_\mu, X_\nu] = iX^\kappa U^\lambda \epsilon_{\mu\nu\kappa\lambda} \ell'^2_P \tag{6}$$

X are Hermitian operators on "bodies." By this we mean objects with large mass so the effects of standard quantum mechanics are negligible compared to those of this new commutator. We also require that the separation between bodies be large enough for the effects of curved spacetime to be negligible. The eigenvalue of X is the location x. U is 4-velocity: $\partial X/c\partial t$, and $\epsilon_{\mu\nu\kappa\lambda}$ is antisymmetric 4-Tensor. The form is covariant and describes the quantum relationship between two timelike trajectories.

In the rest frame, the commutator simplifies to

$$[X_i, X_j] = iX_k \epsilon_{ijk} \ell'^2_P \tag{7}$$

This Planck scale quantum algebra for position operators in three dimensions is similar to the angular momentum algebra, with x in place of J and leads to uncertainty in transverse position after propagating distance D:

$$\langle x_\perp^2 \rangle = D\ell'_P \tag{8}$$

The uncertainty increases with separation D. This "new" quantum departure from classical geometry is purely transverse to the propagation direction.

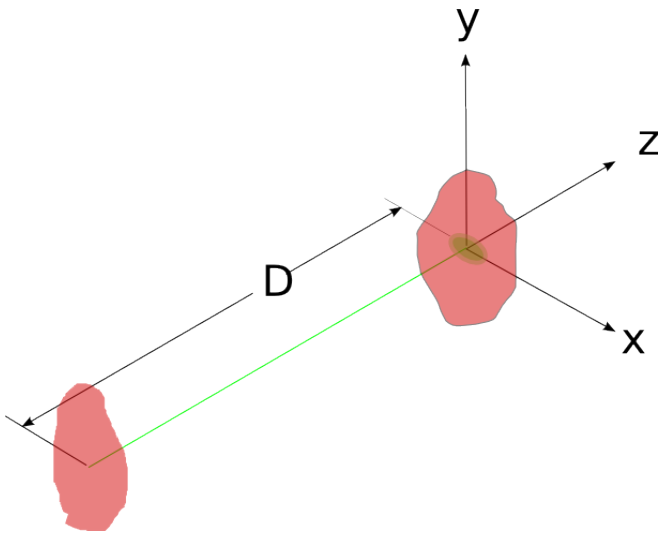

Figure 2: For two objects separated by distance D along the z axis, the transverse uncertainty (in x and y) given by Equation 8 is $\langle x_\perp^2 \rangle = D\ell'_P$. In the Fermilab Holometer we treat the propagation of a photon state in this fashion. Uncertainty in the transverse position at the beam splitter leads to fluctuations in the signal at the dark port which we call "Holographic noise."

Normalization

We have used the primed variable ℓ'_P as the relevant scale for this new uncertainty due to quantum geometry. Calculating the number of degrees of freedom for two bodies confined inside a sphere of radius R allows us to express ℓ'_P in terms of ℓ_P, the Planck length of Equation 1.

Define the state $|d\rangle$ as two bodies separated by distance $D = d\ell'_P$. Then

$$|X|^2|d\rangle = d(d+1){\ell'_P}^2|d\rangle. \tag{9}$$

Consider the separation between two objects, as in Figure 2. For a given separation D, there are $2d+1$ states.

In a sphere, values d are allowed such that $0 \leq d \leq R/\ell'_P$. Each one of these has $2d+1$ states. So the number of states in a 3-sphere of radius R is

$$N_{3S} = \sum_{d=0}^{R/\ell'_P} 2d+1 = d(d+1) \rightarrow (R/\ell'_P)^2 \quad \text{for } R \gg \ell'_P. \tag{10}$$

For the same sphere Verlinde [9] calculates the number of states. Equating the results of Equations 10 and 5 yields

$$\ell'_P = \ell_P / 2\sqrt{\pi}, \tag{11}$$

where ℓ_P is the standard Planck length, 1.6×10^{-35} meters. The normalization is a parameter-free prediction of the magnitude of this effect.

Macroscopic Effect

Consider an interferometer in the coordinate system of Figure 3. The input beam enters an interferometer in the positive x_1 direction and interacts with the beam splitter located at the origin. The photon state splits, propagates in the positive x_1 and x_2 directions, interacts with the two end mirrors (located at distances D_1 and D_2 on the two axes) and returns in the negative x_1 and x_2 directions, recombining at the beam splitter.

The probability that the combined state propagates in the negative x_1 direction or the negative x_2 direction depends on the path length difference $\Delta \equiv D_2 - D_1$. $\langle x_\perp^2 \rangle$ for the two propagation directions changes Δ with a variance of

$$\sigma_\Delta^2 = N_V \langle x_\perp^2 \rangle = N_V D \ell'_P. \tag{12}$$

We use Equation 8 to account for the error in distance in one direction (x_1, for example) due to the perpendicular uncertainty in the other direction (x_2). The factor N_V may be either 1 or 2, and we leave it as a parameter here.

The detector measures photons which exit the interferometer in the negative x_2 direction. The raw data collected is the time series of voltages. (For the Fermilab Holometer, we sample at 100 MHz.) From the optical wavelength and response of the photo detectors, we convert these voltages to a series of measurements of Δ[meters] as a function of time.

We treat $\Delta(t)$ as a stationary random process and adopt the notation of Bendat and Piersol [11] section 5.1.1. The autocorrelation function for $\Delta(t)$ is

$$R_{\Delta\Delta}(\tau) = E[(\Delta(t))(\Delta(t+\tau))] \tag{13}$$

where $E[]$ is the expected value of the function.

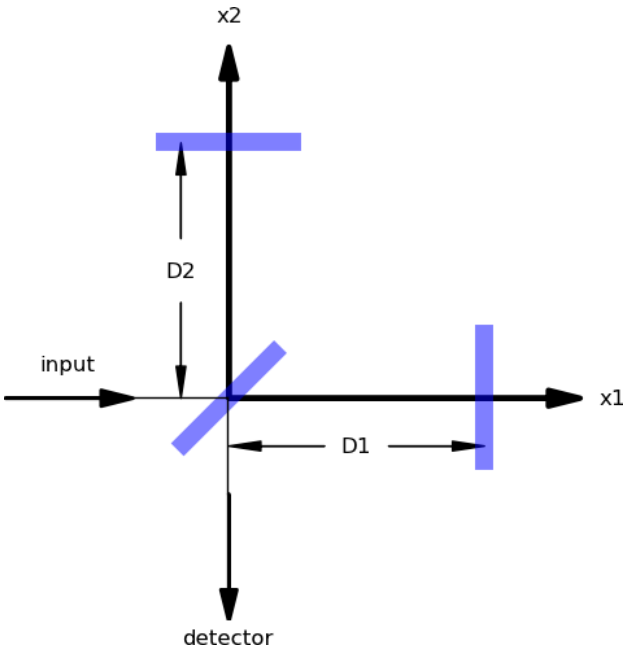

Figure 3: Coordinate system for one interferometer, top view. For the Fermilab Holometer, $\hat{x}_1$ is the Easting direction, $\hat{x}_2$ is the Northing direction, and $\hat{x}_3$ is up. The path length difference $\Delta \equiv D_2 - D_1$ is controlled at low frequencies to "lock" the interferometer at a constant power output to the detector. Holographic noise adds additional uncertainty to the measurement of Δ, with the variance σ_Δ^2 given by Equation (12)

At zero time lag the autocorrelation function is the variance, given by Bendat and Piersol [11] Equations 5.4 and 5.8 with mean value of zero:

$$R_{\Delta\Delta}(\tau = 0) = \sigma_\Delta^2 \tag{14}$$
$$= N_V D \ell'_P. \tag{15}$$

Define a critical time lag τ_c such that $R_{\Delta\Delta}(\tau)$ is zero for $\tau \geq \tau_c$. We also propose linear interpolation between $\tau = 0$ and $\tau = \tau_c$:

$$R_{\Delta\Delta}(\tau) = (1 - |\tau|/\tau_c) N_V D \ell'_P \quad \text{for } 0 \leq |\tau| \leq \tau_c \tag{16}$$
$$= 0 \quad \text{for } \tau_c < |\tau|.$$

Note that for a stationary random process, $R_{\Delta\Delta}(\tau) = R_{\Delta\Delta}(-\tau)$.

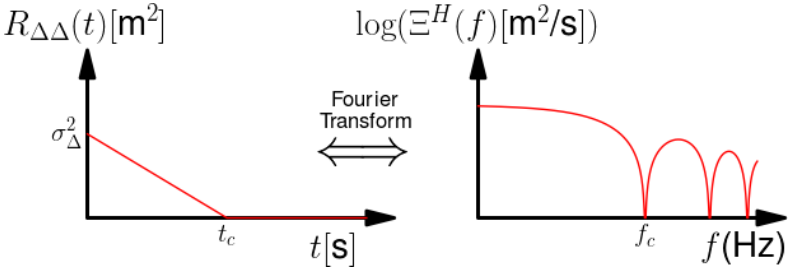

Figure 4: Relation between the autocorrelation function and power spectral density for Holographic noise.

The critical time lag is related to the time of flight of the photon state in the interferometer. For the round trip between beam splitter and end mirror, $\tau_c = 2D/c$. However, the transverse position error may depend only on the propagation from the end mirror to the beam splitter, so we define

$$\tau_c = N_\tau D/c \tag{17}$$

The factor N_τ is either 1 or 2, depending on whether the transverse position error depends on propagation from the end mirror to the beam splitter, or the entire round trip, respectively.

Signal to Noise Ratio: One Interferometer

Starting with the autocorrelation function of Equation 16 we use standard signal processing techniques to calculate the signal to noise ratio.

Following Bendat and Piersol [11] eq. 5.34, the one-sided autospectral density function (power spectral density) $\Xi^H(f)$ is the cosine transform of $R_{\Delta\Delta}(\tau)$. Here we use the superscript H to designate the Holographic noise. Later, we will use superscript P to designate photon noise with Poisson statistics, the dominant background to measuring Holographic noise.

$$\Xi^H(f) = 4\int_0^\infty R_{\Delta\Delta}(\tau)\cos(2\pi f\tau)\,d\tau \tag{18}$$

$$= 4\ell'_P N_V D\int_0^{\tau_c}(1-\tau/\tau_c)\cos(2\pi f\tau)\,d\tau \tag{19}$$

$$= \frac{\ell'_P N_V D}{\pi^2\tau_c}\frac{1}{f^2}(1-\cos(2\pi f\tau_c)) \tag{20}$$

The low-frequency limit (using l'Hôpital's rule) is

$$\lim_{f\to 0}\Xi^H(f) = \frac{\ell'_P N_V D}{\pi^2\tau_c}\lim_{f\to 0}\frac{1}{f^2}(1-\cos(2\pi f/f_c)) \tag{21}$$

$$= \frac{N_V N_\tau \ell_P D^2}{c\sqrt{\pi}} \tag{22}$$

For frequencies > 10 kHz background noise is dominated by photon statistics which, for laser light, follows Poisson statistics[12]. Increasing the number of photons per second reduces the Poisson noise contributions to σ_Δ. For a Poisson process with rate $\dot{n}$ photons/second, the power spectrum of the relative intensity is

$$\phi(f)_{\text{Poisson}} = \sqrt{\frac{1}{\dot{n}}}\ \text{Radians}/\sqrt{\text{Hz}} \tag{23}$$

$$= \sqrt{\frac{E_\gamma}{P_{BS}}}\ \text{Radians}/\sqrt{\text{Hz}} \tag{24}$$

Expressed as root-mean square fluctuation in Δ[meters]:

$$\sqrt{\Xi^P(f)} = \sqrt{\frac{hc\lambda_\gamma}{4\pi^2 P_{BS}}}\ \text{meters}/\sqrt{\text{Hz}}. \tag{25}$$

This is white noise, constant at all frequencies. Compare this to the shape of Holographic noise in Figure 4.

To estimate the integration time we need to distinguish Holographic noise from Poisson noise. Calculate the Signal to Noise ratio for $f \to 0$.

$$S/N = \frac{\sqrt{\Xi^H(f\to 0)}}{\sqrt{\Xi^P(f)}} = D\sqrt{\frac{\ell_P P_{BS}}{\lambda_\gamma}}\sqrt{N_V N_\tau}\frac{2\pi^{3/4}}{c\sqrt{h}} \tag{26}$$

Each of the interferometers in the Fermilab Holometer has these parameters:

$$D = 40 \text{ meters (Arm Length)} \tag{27}$$

$$\lambda_\gamma = 1.064\times 10^{-6} \text{ meters (wavelength of infrared laser)} \tag{28}$$

$$P_{BS} = 1\times 10^3 \text{ watts (Power on Beam Splitter).} \tag{29}$$

For this design and assuming $N_V = 2$ and $N_\tau = 2$, the above quantities are

$$\sqrt{\Xi^H(f \to 0)} = 1.39 \times 10^{-20} \text{ meters}/\sqrt{\text{Hz}} \tag{30}$$

$$\sqrt{\Xi^P(f)} = 1.64 \times 10^{-18} \text{ meters}/\sqrt{\text{Hz}} \tag{31}$$

$$S/N = 0.6\% \tag{32}$$

One way to improve the S/N ratio is to increase the power on the beam splitter P_{BS}. At more than several kilowatts, however, thermal distortions on the beam splitter limit the performance of the interferometer. A second way to improve S/N is increasing the arm length D also. However, even with the length of the most ambitious optical interferometers (for example, LIGO [13] has $D = 4$ km) the S/N ratio is still < 1.

Signal to Noise Ratio: Correlation of Two Interferometers

We improve the S/N ratio by measuring $\Delta(t)$ for two independent interferometers. $\Xi^O_{0,1}$ is the observed cross correlation of the two time streams $\Delta_0(t)$ and $\Delta_1(t)$, with:

$$\Xi^O_{0,1}(f) = \Xi^H_{0,1}(f) + \Xi^P_{0,1}(f) \tag{33}$$

Why is Holographic noise correlated? Figure 5 shows two configurations we use to probe Holographic noise. Each photon measures Δ for an interferometer. The variations in Δ we are concerned with are not a property of the photon, or of the interferometer's mirrors, but rather are due to the measurement of the location (x_1 and x_2) of the beam splitter by the photon state. Our conjecture is that this is a property of spacetime in which measurements occur. For the nested configuration, the two interferometers are embedded in the same volume of spacetime, so the fluctuations in Δ_0 are correlated with fluctuations in Δ_1. In the nested configuration the separation between the two interferometers (0.6 meters) $\ll D = 40$ meters so for these estimates of the S/N ratio we set the correlation coefficient to 1.

Our experiment allows us to switch between the "nested" and the "back-to-back" configurations. For this we do not need to move the electronics, detectors, digitizers, or computers. The only change in the optics is the rotation of one beam splitter by 90 degrees, and the use of a different end mirror in one of the interferometers. The modulation of the correlation coefficient between the two configuration of Figure 5 is an important signature of Holographic noise.

The power spectrum $\Xi^H(f)$ is the same for the two interferometers. The cross correlation of Holographic noise is

$$\Xi^H_{0,1}(f) = \Xi^H(f) \tag{34}$$

where $\Xi^H(f)$ is given by Equation 20 for all f with the low-frequency limit of Equation 22.

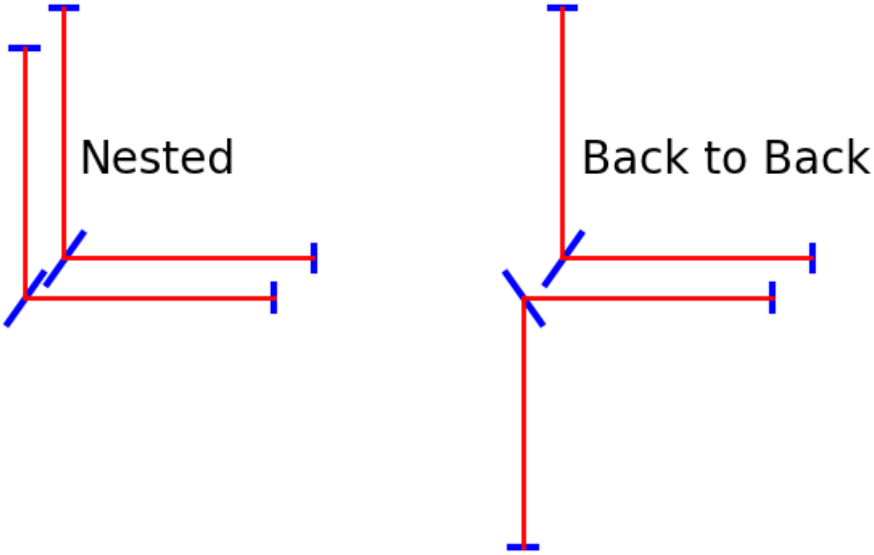

Figure 5: Configurations of two interferometers in the Fermilab Holometer. We measure $\Delta(t)$ for the two interferometers independently and calculate the cross correlation $\Xi^O_{(0,1)}$ of $\Delta_0(t)$ and $\Delta_1(t)$. For clarity in this diagram, we show the separation between interferometers expanded by a factor of ten.

The Poisson noise in the two interferometers is uncorrelated. Separate lasers feed each interferometer, and we keep the two light paths completely isolated. We average the cross correlation for N_S independent samples. The sampling time t_S is the time between independent samples, the round trip time of flight $2D/c$. For an integration time t_I we have

$$N_S = t_I/t_S \tag{35}$$

In calculating the average, each term of the sum has the same magnitude, but random phase. For a random walk in two dimensions, after

N unit-length steps, the root mean square of the distance traveled [14] is $|z|_{RMS} = \sqrt{N}$. The average cross correlation of the Poisson noise is

$$\Xi^P_{0,1}(f) = \Xi^P(f)/\sqrt{N_S}. \tag{36}$$

Now we find the integration time T_I by equating the cross correlations of the Poisson noise and Holographic noise.

$$\Xi^P_{0,1}(f) = \Xi^H_{0,1}(f \to 0) \tag{37}$$

$$\Xi^P(f)/\sqrt{N_S} = \Xi^H(f \to 0) \tag{38}$$

$$\sqrt{\frac{2D}{cT_I}}\frac{hc\lambda_\gamma}{4\pi^2 P_{BS}} = \frac{N_V N_\tau \ell_P D^2}{c\sqrt{\pi}} \tag{39}$$

Solving for T_I:

$$T_I = \left(\frac{\lambda^2}{P^2_{BS}D^3}\right)\left(\frac{1}{N_V^2 N_\tau^2}\right)\left(\frac{1}{\ell_P^2}\right)\left(\frac{h^2c^3}{8\pi^3}\right) \tag{40}$$

The first term illustrates design strategies for the apparatus. Integration time is reduced by laser power squared and by arm length cubed. It is also reduced by a shorter laser wavelength squared, but we trade that off with the ease of building power recycled interferometers in the infrared. In the second term, we see the two factors N_V and N_τ. In these calculations, we set these both to 2. Interpretations which have these as 1 increases the integration time by their product squared. Note that for $N_\tau = 1$, the critical frequency $f_c = 1/\tau_c$ in Figure 4, Equation 17 changes by a factor of two. The third term, Planck length squared, is powerful. Two chief ideas behind the Fermilab Holometer overcome this scale: $\langle x^2_\perp \rangle = D\ell_P'^2$ and Holographic noise is coherent on length scales $\sim D$. A large value of D amplifies effects from the Plank length scales to macroscopic length scales.

For the Fermilab Holometer, an integration time of 206 seconds achieves a S/N ratio of one for the cross correlation between two interferometers. An important caveat is that this estimate does not include additional noise due to imperfections in the optics of an interferometer or misalignment. Our current activities will quantify and ameliorate these effects.

Summary

We have combined recent theoretical ideas and experience with operating Michelson interferometers to design an experiment, the Fermilab Holometer, which is sensitive to macroscopic effects predicted by quantum geometry at the Planck length scale. This relies on "new" theoretical ideas:

- measurement of the location of an object in two orthogonal directions obeys a commutator $[X_i, X_j] = iX_k\epsilon_{ijk}\ell'_P$;
- considerations of entropy from the Holographic Principle and the number states of separation of two bodies with with Holographic uncertainty normalizes the length scale $\ell'_P = \ell_P/2\sqrt{\pi}$ where $\ell_P = \sqrt{\hbar G/c^3}$ is the Planck length;
- Holographic uncertainty adds noise to measurements of the location of the beam splitter in a Michelson interferometer;
- The autocorrelation function $R_{\Delta\Delta}(\tau)$ for Holographic noise in one interferometer falls from $R_{\Delta\Delta}(0) = \sigma^2_\Delta$ to 0 at $\tau = \tau_c$;
- Holographic noise of two co-located interferometers is correlated and depends on the overlapping spacetime volume.

We have designed, assembled and are currently commissioning the Fermilab Holometer. We will be sensitive to the macroscopic effects of these ideas:

- magnitude of the cross correlation;
- spectral shape of the cross correlation;
- modulation of the cross correlation with the configuration of the interferometers.

Acknowledgments

I thank the entire Holometer collaboration [15], especially C. Hogan and S. Meyer for discussions of these ideas. Fermilab is operated by Fermi Research Alliance, LLC under Contract No. DE-AC02-07CH11359 with the United States Department of Energy.

I also thank the organizers of the Time and Matter 2013 Conference.

References

[1] Craig J. Hogan, *Measurement of quantum fluctuations in geometry* Phys. Rev. D 77 (10) (2008), arXiv:0712.3419.

[2] *Indeterminacy of Holographic Quantum Geometry*, Craig J. Hogan, Phys. Rev. D 78, 087501 (2008).

[3] Craig J. Hogan, *Interferometers as Probes of Planckian Quantum Geometry*, arXiv:1002.4880.

[4] Craig J. Hogan, *Macroscopic Quantum Geometry*, arXiv:1204.5948.

[5] K. A. Tomlin, *NATURAL SYSTEMS OF UNITS. To the Centenary Anniversary of the Planck System*, `http://www.ihst.ru/personal/tomilin/papers/tomil.pdf`.

[6] S. W. Hawking, *Gravitational Radiation from Colliding Black Holes"*, Physical Review Letters, 26, 1344 (1971).

[7] P. Majumdar, *Black Hole Entropy and Quantum Gravity*, arXiv:gr-qc/9807045v3.

[8] R. Bousso, *The holographic principle*, Review of Modern Physics, 74(3):825-874.

[9] E.P. Verlinde. *On the Origin of Gravity and the laws of Newton*, JHEP 2011:29.

[10] Gerard 't Hooft. *The Holographic Principle*, arXiv:hep-th/0003004v2 (May 2000).

[11] Julius S. Benda and Allan G. Piersol, *Random Data: Analysis and Measurement Procedures*, Fourth Edition, Wiley (2010).

[12] R.J. Glauber, *Coherent and incoherent states of radiation field*,Phys. Rev. 131 (1963) 2766-2788.

[13] *Web site for Laser Interferometer Gravitational-Wave Observatory*, `http://www.ligo.caltech.edu/`.

[14] Weisstein, Eric W. *Random Walk–2-Dimensional*, From MathWorld–A Wolfram Web Resource. `http://mathworld.wolfram.com/RandomWalk2-Dimensional.html`.

[15] *Web site for The Fermilab Holometer*, `http://holometer.fnal.gov`